論文 / 著書情報
Article / Book Information

Title	FRAGILITY EVALUATION OF BUCKLING RESTRAINED BRACES FOR LONG-PERIOD GROUND MOTIONS AND HUGE SEISMIC LOADS
Authors	Takuya Ueki, Takumi Ishii, Kazuaki Miyagawa, Daiki Sato, Haruyuki Kitamura
Citation	Proceedings of the 10th Pacific Structural Steel Conference, , , pp. 843-848
Pub. date	2013, 10

Fragility Evaluation of Buckling Restrained Braces for Long-period Ground Motions and Huge Seismic Loads

Takuya Ueki; Takumi Ishii
Civil Engineering Research Department
JFE Steel Corporation, 1-1 Minamiwataridamachi, Kawasaki-ku, Kawasaki, Japan
t-ueki@jfe-steel.co.jp; taku-ishii@jfe-steel.co.jp

Kazuaki Miyagawa
Metal Building Construction Department
JFE Civil Engineering & Construction Corporation, 2-17-4 Kuramae, Taitou-ku, Tokyo, Japan
miyagawa@jfe-civil.com

Haruyuki Kitamura
Department of Architecture
Tokyo University of Science, 2641 Yamazaki Noda-shi Chiba, Japan
kita-h@rs.noda.tus.ac.jp

Daiki Sato
Hyogo Earthquake Engineering Research Center
National Research Institute for Earth Science and Disaster Prevention, 1501-21 Nishikameya Shijimicho-mitsuda, Miki-shi, Hyogo, Japan
daiki-s@bosai.go.jp

Abstract

This paper discusses the damping effects and damage index of buckling restrained braces for long-period ground motions and huge seismic loads. As a result of dynamic loading tests, it was confirmed that buckling restrained braces show high performance in seismic energy absorption for recurrent earthquakes repeated approximately 10 times. Furthermore, a new estimation method for the damage index by using the quantity of total energy absorption and the mean of strain extracted from the seismic response analysis was proposed. The effectiveness of this method was clarified by application to previous experiments.

1. Introduction

The earthquakes that are assumed in Japan are broadly classified into two types. One is a huge subduction-zone earthquake that causes long-period ground motion. As this ground motion is characterized by long duration and little attenuation, seismic energy arrives over a large area. For example, in the 2011 off the Pacific coast of Tohoku Earthquake, buildings in Tokyo and Osaka, which are far from the seismic center, reportedly shook for approximately ten minutes and maximum horizontal displacement reached around 1.0m.

The other type is generated by large inland earthquakes that cause a pulse-like ground motion.

Proceedings of the 10th Pacific Structural Steel Conference (PSSC 2013)
Editors: Richard J. Y. Liew and Siew Chin Lee

ISBN: 978-981-07-7137-9 :: doi:10.3850/978-981-07-7137-9 109

Because this ground motion includes a pulse wave, there is a risk of sudden destruction of buildings by momentary impulse force and large deformation before showing adequate seismic energy absorption. Furthermore, after such large earthquakes, the number of subsequent aftershocks tends to increase. As a result, it is difficult to judge whether continuous use of a building is possible or not even if the building is not destroyed by one earthquake.

Therefore, it is important to evaluate the damage of buildings appropriately after an earthquake occurs. This paper describes a method for judging the damage index of damping devices, which are effective for reducing the damage of the main structure, by using the results of time history response analysis with observed or predicted ground motion.

2. Performance of damping device for repeated ground motions

2.1. Damping effects based on trial design analysis

First, in order to evaluate the effects of the damping device, a time history response analysis of the trial design building was carried out. In this case, the damping device was the buckling restrained brace (hereinafter, BRB) shown in Figure 1. The BRB consists of a cross-shaped axial member using low-yield stress steel LY225 as the energy absorption material and a restrained member using a welded box-section that restricts buckling of the axial member.

The seismic waves used in this analysis were OSA NS and WOS EW, which are assumed to arrive at Osaka in a Nankai Earthquake (huge subduction-zone type earthquake), as long-period ground motion, and JMA KOBE, which was observed at the Kobe Marine Observatory in the 1995 Hyogoken-Nambu Earthquake (inland type earthquake), as a pulse-like ground motion. The energy spectrums for each seismic wave are shown in Figure 2.

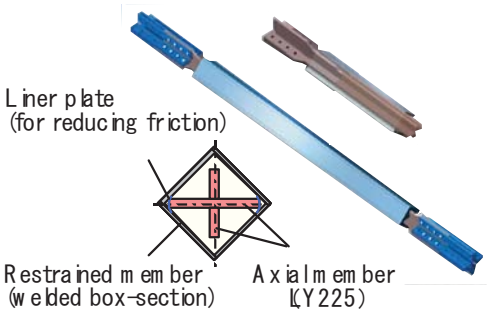

Figure 1: Buckling Restrained Brace (BRB)

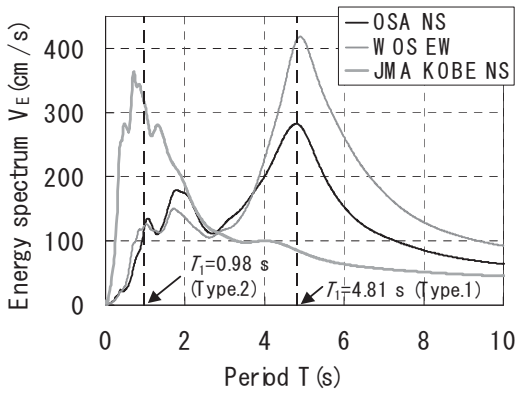

Figure 2: Energy spectrums

The scale of the trial design buildings (Figure 3) in rigid steel frames were decided so that the natural period T_1 of the buildings after BRB installation accorded with the period when the energy spectrum of each seismic wave reached its peak (Figure 2).

Figure 4 shows the distribution of the story drift angle obtained by analysis. Installation of BRB reduced the maximum story drift angle less than the general safety limit (1/100 for OSA NS and WOS EW, 1/75 for JMA KOBE NS). In this case, the required performance of the BRB in seismic energy absorption is expressed by the cumulative plastic deformation ratio η

shown in Table 1 below in comparison with the experimental results. Here, η is defined by dividing the quantity of total energy absorption W (kNm) by yield strength N_y (kN) and yield displacement δ_y (m).

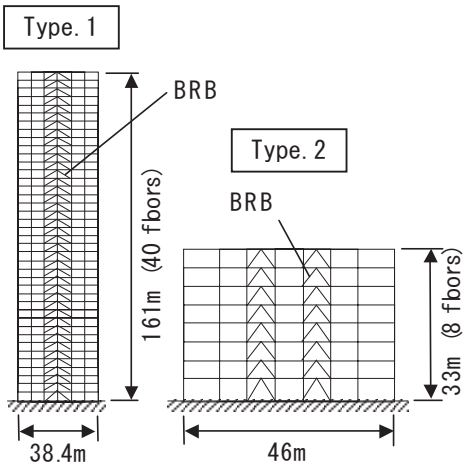

Figure 3: Analytical building model

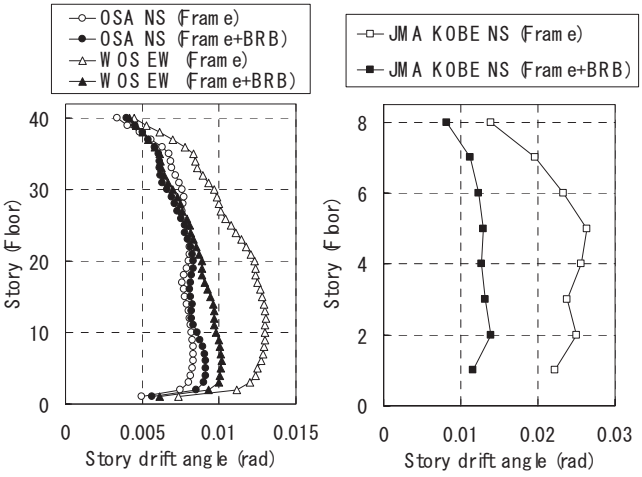

Figure 4: Distribution of story drift angle

2.2. Energy absorption capacity of BRB

In order to clarify the energy absorption capacity of BRB, dynamic loading tests reflecting the foregoing trial design analysis were performed. The shape of the BRB test specimen in Figure 5 is an approximate 2/3 scale model of that used in the analysis. The width thickness ratio of the axial member and the diameter/thickness ratio of the restrained member, which affect the BRB performance, were set to be approximately equal to those in the analysis.

The loading system is shown in Figure 6. The input wave with the actuator is a horizontal response wave in the floors that displayed the maximum story drift angles in the analysis, namely, the 7th floor for OSA NS and WOS EW and the 2nd floor for JMA KOBE NS. However, the amplitude of the waves was adjusted so that the strain of the axial member in the experiment equaled that in the analysis.

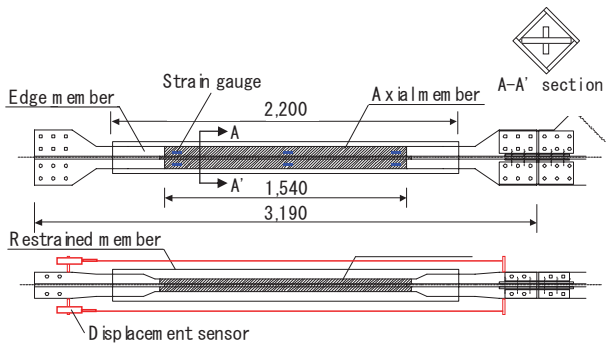

Figure 5: Test specimen

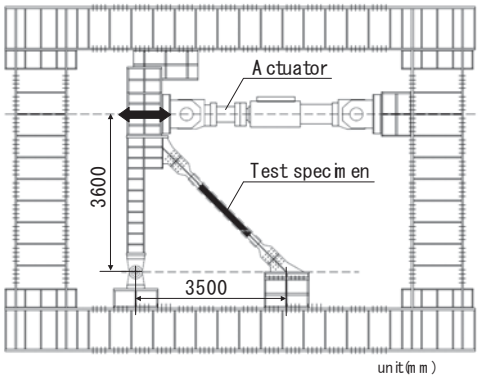

Figure 6: Loading system

The response strain histories of the BRB axial member used to compare the experiment with the analysis for each 1st seismic wave are shown in Figure 7. Because the experimental and analytical histories showed close agreement, it is clear that the experiment could reproduce the analysis appropriately.

The stress-strain relationships are shown in Figure 8. As a result of repeating input of the same seismic wave 10 times, in the case of OSA NS and WOS EW, the maximum stress decreased slightly, but there were no significant differences in the stable fusiform hysteresis loops between the 1st and 10th cycles. On the other hand, with JMA KOBE NS, the hysteresis loop showed a butterfly shape as the out-of-plane in the axial member progressed, but the stress at the time of maximum strain was recovered.

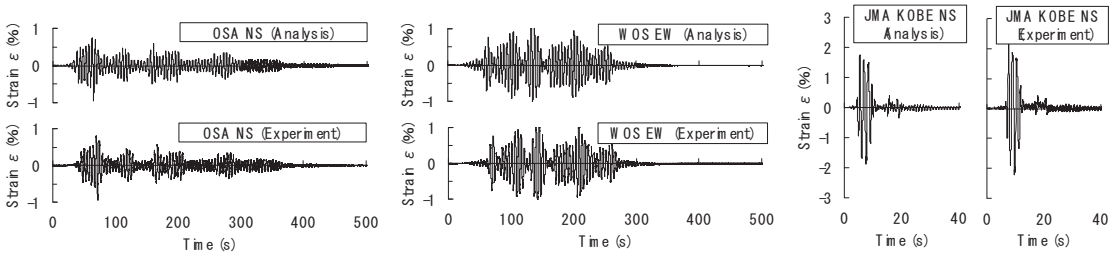

Figure 7: Time histories of BRB strain

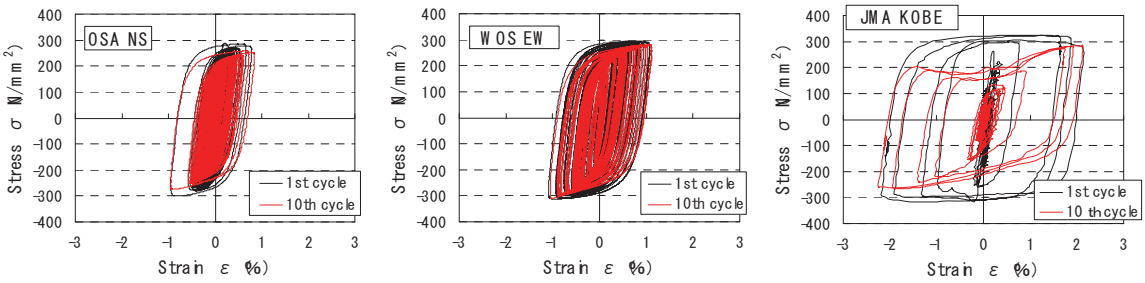

Figure 8: Stress-strain relationships

Cyclic loading was continued, and the axial member finally reached ductile fracture under tension load. In this connection, the amplitude of the input waves for OSA NS and WOS EW were amplified to 1.5 times after the 10th cycle. The number of cycles and cumulative plastic deformation ratio η until one cycle before fracture are shown in Table 1. As the experimental value of η exceeded that required by the analysis, it is clear that BRB has high performance in seismic energy absorption.

Table 1: Result of tests

Seismic waves	Number of cycles		Cumulative plastic deformation ratio, η	
	Amplification ×1.0	Amplification ×1.5	Experiment	Analysis
OSA NS	10	2	5,502	127
WOS EW	10	1	8,807	298
JMA KOBE NS	11	—	3,050	215

3. Evaluation of damage index of BRB

3.1. Calculation by Miner's law

This section proposes an estimation method for the damage index of BRB. One general method for evaluating fatigue damage is Miner's law. In applying Miner's law, it is necessary to grasp the relationship between the strain range $\Delta\varepsilon$ and the limit number of repeated cycles N_{cr} by performing constant amplitude loading tests. The fatigue curve of BRB that was used in the tests presented here is expressed in Equation (1).

$$\Delta\varepsilon = 15.83 \times N_{cr}^{-0.44} \tag{1}$$

Secondly, the random response wave must be divided into the 1/2 wavelength, which is considered to be part of the constant amplitude wave. Here, the amplitude method and rain flow method are adopted as division methods for the random wave. Figure 9 shows the frequency distribution of the 1/2 wavelength used to constitute the response strain wave for OSA NS. Here, the elastic strain range ($\Delta\varepsilon \leqq 0.2\%$) is omitted. Regardless of the method used, the results were substantially the same.

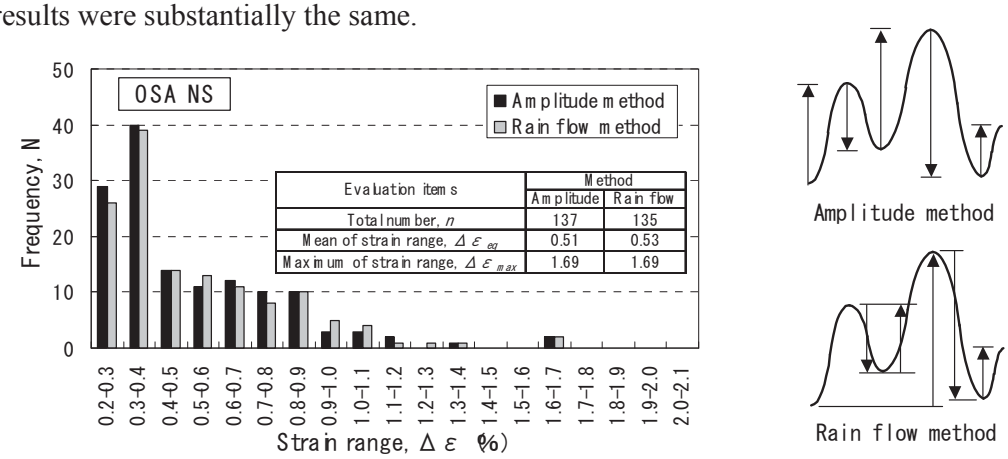

Figure 9: Frequency distribution of 1/2 wavelength (OSA NS)

The damage index for the individual 1/2 wavelength is expressed by $1/(2\times N_{cr})$. Therefore, the total damage index D of a seismic wave is expressed by Equation (2).

$$D = \frac{1}{2\times_1 N_{cr}} + \frac{1}{2\times_2 N_{cr}} + \cdots + \frac{1}{2\times_n N_{cr}} = \sum_{i=1}^{n} \frac{1}{2} \cdot \left(\frac{15.83}{\Delta\varepsilon_i} \right)^{-1/0.44} \tag{2}$$

Here,

n : Total number of 1/2 wavelengths included in seismic wave

$\Delta\varepsilon_i$: Strain range for i'th 1/2 wavelength

The damage index D obtained by using Miner's law for each seismic wave are shown in the (i) column of Table 2. Although there is some estimation error, D is calculated as almost 1.0 in the cycle before that leading to fracture.

3.2. New estimation method of damage index

A new method for evaluating the damage index in consideration of energy absorption is proposed. In this method, a random wave is converted into a constant amplitude wave so that the quantity of total energy absorption becomes equivalent, and the mean of the strain range $\Delta\varepsilon_{eq}$ extracted from the response wave is used for amplitude. The number of cycles N_{eq} for the converted constant amplitude wave is expressed by Equation (3).

$$N_{eq} = \frac{\eta}{\eta_{eq}} \tag{3}$$

Here,

η : Cumulative plastic deformation ratio for seismic wave

η_{eq} : Cumulative plastic deformation ratio for 1 wavelength of $\Delta\varepsilon_{eq}$

The relationship between η_{eq} and $\Delta\varepsilon_{eq}$ that was obtained by constant amplitude loading tests is expressed by Equation (4).

$$\Delta\varepsilon_{eq} = 0.184 \cdot \eta_{eq}^{0.717} \tag{4}$$

Using Equations (1), (3) and (4), the total damage index D is finally expressed as shown in Equation (5).

$$D = \frac{N_{eq}}{N_{cr}} = \frac{\eta}{\left(\Delta\varepsilon_{eq}/15.83\right)^{-1/0.44} \cdot \left(\Delta\varepsilon_{eq}/0.184\right)^{1/0.717}} = \frac{\eta}{5642 \cdot \Delta\varepsilon_{eq}^{-0.878}} \tag{5}$$

Therefore, the total damage index D can be calculated if $\Delta\varepsilon_{eq}$ and η are given by the time history response analysis for any seismic wave or building. The value of the damage index D obtained by applying Equation (5) to each previous test result are shown in the (ii) column of Table 2. The damage index D calculated using the proposed method is approximately equal to that calculated using Miner's law, except for JMA KOBE NS. The reason why D for JMA KOBE NS was small is because it was possible to reflect the change in the hysteresis loop due to repetition as shown in Figure 8. In other words, the damage index D calculated using the Miner's law tends to give an excessive evaluation in case of a pulse-like ground motion that causes large strains of BRB. In comparison with a fatigue curve, the number of cycles evaluated by the proposed method is shown in Figure 10. These plots are at the position that is approximately near to a fatigue curve on a logarithm, demonstrating the effectiveness of this method.

Table 2: Comparison of damage index

Damage index	Seismic waves		
	OSA NS	WOS EW	JMA KOBE NS
ⅰ .Miner's law	0.71	1.54	**1.31**
ⅱ .Proposed method	0.67	1.65	**0.81**

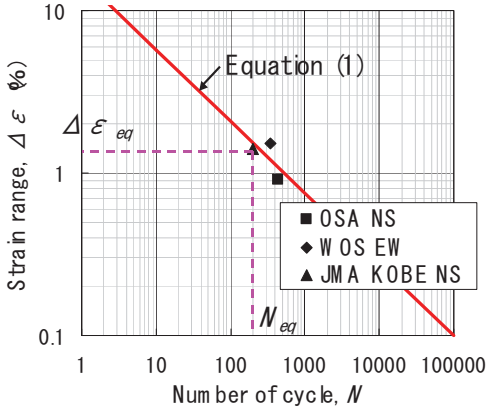

Figure 10: Estimated results

4. Conclusion

The BRB discussed in this paper can be removed easily from the main structure. By using this new estimation method, it is possible to judge the appropriate timing for BRB exchanges, enabling continuous use of the building after an earthquake occurs.

Further investigation of the cause of error is needed, including, for example, study of the influence of the order in which different amplitudes are received.

References

Kamae K, Kawabe H and Irikura K. (2004). *Strong Ground Motion Prediction for Huge Subduction Earthquakes Using a Characterized Source Model and Several Simulation Techniques*, 13th WCEE, Canada. paper No.655.

Koyama. M and Aoki. H. (2002). *Study on the Par ameter of Eval uating Cumulative Damage of Alternative Deformed Steel Members*, AIJ, Japan. pp. 159-166.